Tripartite motif containing 33 demonstrated anticancer effect by degrading c-Myc: Limitation of glutamine metabolism and proliferation in endometrial carcinoma cells

YUE QI*, NINGYE MA* and JIN ZHANG

Department of Obstetrics and Gynecology, Shengjing Hospital of China Medical University, Shenyang, Liaoning 110022, P.R. China

Received June 12, 2023; Accepted September 6, 2023

DOI: 10.3892/ijo.2023.5581

Abstract. Tripartite motif containing 33 (TRIM33) has been reported to be involved in various tumor progression. However, its role in endometrial carcinoma (EC) remains to be elucidated. By mining the publicly available databases UALCAN and TIMER, low expression of TRIM33 was found in tumor tissues of EC patients. Clinically, downregulation of TRIM33 in EC tissues was positively correlated with the extensive muscle invasion and poor differentiation grade. *In vitro*, experiments performed on human HEC-1-A and AN3CA cells showed that overexpression of TRIM33 inhibited the proliferation, migration and invasion of EC cells, whereas TRIM33 knockdown resulted in the opposite results. Furthermore, upregulation of TRIM33 significantly inhibited the glutamine uptake and decreased the intracellular glutamate in EC cells, which is evidenced by the reduction of solute carrier family 1 member 5 and glutaminase. *In vivo*, TRIM33 also dramatically inhibited tumor growth and glutamine metabolism. Additionally, co-immunoprecipitation assay confirmed the interaction between TRIM33 and c-Myc. Overexpression of TRIM33 could reduce the protein stability of c-Myc by promoting its degradation. In addition, upregulation of c-Myc could reverse the effects of TRIM33 on EC cells. Together, the present study demonstrated that TRIM33 acted as a tumor suppressor in EC, which is manifested in its inhibition of glutamine metabolism and cell growth via promoting c-Myc protein degradation.

Correspondence to: Dr Jin Zhang, Department of Obstetrics and Gynecology, Shengjing Hospital of China Medical University, 39 Huaxiang Road, Shenyang, Liaoning 110022, P.R. China
E-mail: 2019140256@cmu.edu.cn

*Contributed equally

Key words: tripartite motif containing 33, glutamine metabolism, c-Myc, endometrial carcinoma

Introduction

Endometrial carcinoma (EC) is the result of the abnormal growth of cells in the lining of the uterus or womb, which commonly occurs following menopause (1). In 2022, cancer statistics by the American Cancer Society showed that EC newly occurred in ~65,950 women and the fatality rate exceeded 4% (2). Although the incidence rate of EC appears to have stabilized in recent years, the aging of population, the rising obesity rates and the continued declines in the fertility rate may also contribute to the increase in EC incidence. Therefore, exploring reliable and potential therapeutic targets is essential to treating patients with EC.

Tripartite Motif Containing 33 (TRIM33) is a chromatin-associated transcriptional repressor with an N-terminal RING domain and a C-terminal plant homeodomain (PHD)-bromodomain cassette structure, which interacts with post-translationally modified histone tails (3). Studies have confirmed that TRIM33 facilitates DNA repair (4), regulates mitosis (5) and controls transcription elongation (6). A recent study reported that TRIM33 promotes prostate tumor growth by stabilizing Skp2-mediated androgen receptor degradation (7). By contrast, Herquel *et al* (8) demonstrated that TRIM33 inhibits the progress of murine hepatocellular carcinoma by forming regulatory complexes in combination with other transcriptional cofactors. Overexpression of TRIM33 also suppresses the growth of renal clear cell carcinoma both *in vitro* and *in vivo* (9). However, the expression and function of TRIM33 in EC are not yet fully elucidated.

c-Myc, a helix-loop-helix leucine zipper transcription factor, dimerizes with its partner protein Max to bind specific DNA sequences and transactivate the downstream genes (10). c-Myc serves a vital role in cell growth, differentiation and apoptosis and its abnormal expression is associated with oncogenesis (11). Previous studies showed that c-Myc was highly expressed in various cancers, such as EC (12), prostate cancer (13), epithelial ovarian carcinoma (14) and colorectal cancer (15). Inhibition of c-Myc exhibits a significant anti-proliferative effect and persistent tumor regression (16). In addition, c-Myc can enhance tumor glutamine metabolism to promote tumor cell growth (17,18). Although a previous study suggested that TRIM33 could inhibit the expression of

c-Myc (9), whether TRIM33 participates in the progress of EC by directly affecting the stability of c-Myc deserves further exploration.

The present study aimed to explore the role of TRIM33 in EC cell growth and glutamate metabolism. Furthermore, *in vitro* cell experiments (HEC-1-A and AN3CA) and *in vivo* xenograft model in BALB/c nude mice were established to investigate its potential mechanisms.

Materials and methods

Clinical samples. The present study used 81 paraffin-embedded tumor tissues and fresh-frozen tumor/normal endometrium tissues (23/20) from patients with EC at the Shengjing Hospital of China Medical University. Informed consent was obtained from the participants. All experiments performed in this study were completed in accordance with the *Declaration of Helsinki* as revised in 2013 and approved by the ethics committee of Shengjing Hospital of China Medical University (approval no. 2018PS251K). Clinicopathological parameters of patients are given in Table I.

Cell culture. Human EC cell lines (HEC-1-A and AN3CA) were purchased from iCell Bioscience Inc. Cell lines were identified by STR profiling. HEC-1-A cells were cultured in the McCoy's 5A medium (Wuhan Servicebio Technology Co., Ltd., China) supplemented with 10% fetal bovine serum (FBS; Zhejiang Tianhang Biotechnology Co., Ltd.). AN3CA cells were cultured in Minimum Essential Medium (MEM, Beijing Solarbio Science & Technology Co., Ltd.) supplemented with 10% FBS. Both cell lines were cultured at a condition of 37˚C and 5% CO_2.

Plasmid and lentivirus transduction. To overexpress c-Myc, cells were seeded in 6-well plates at a density of $5x10^5$ cells/well and incubated in a 37˚C, 5% CO_2 incubator for 24 h, followed by transfection for 48 h at 37˚C with 2.5 μg pDONR223-c-Myc plasmid (cat. no. G152835; Youbao Biotech) using Lipofectamine® 3000 (Invitrogen; Thermo Fisher Scientific, Inc.) according to the manufacturer's protocol. Short-hairpin (sh)RNAs targeting TRIM33 (TRIM33-1: 5'-GGUAUGUAC UAGUUGUGAAGA-3'; TRIM33-2: 5'-CCAGCAAGUUGG UGUAAUACG-3') or its negative control (shNC: 5'-UUC UCCGAACGUGUCACGU-3') were constructed by General Biology (Anhui) Co., Ltd. These shRNAs were inserted into pLVX-shRNA1 lentivirus vector (Lv; cat. no. VT1456; Youbao Biotech) to construct Lv-TRIM33-shRNA1, Lv-TRIM33-shRNA2 and Lv-shNC. To overexpress TRIM33, the coding sequence of TRIM33 was inserted into the pLVX-IRES-puro lentivirus vector (cat. no. VT1464; Youbao Biotech) to construct Lv-TRIM33-OV. Lentivirus was packaged in 293T cells according to the manufacturer's protocol. At 72 h later, the virus supernatant was collected and used for cell infection. Briefly, HEC-1-A and AN3CA cells were seeded in 6-well plates at a density of $1x10^5$ cells/well. Subsequently, 10 μl of virus (titer=$1x10^8$ TU/ml) was added to the culture medium of HEC-1-A cells while 20 μl virus was added to the culture medium of AN3CA cells. After being transfected for 48 h at a 37˚C in a 5% CO_2 incubator, 3 and 2 μg/ml puromycin were added into the culture medium of HEC-1-A and AN3CA cells, respectively. The stable express cells were obtained by puromycin selection for 7 days.

CCK-8 assay. Cell viability was evaluated by a commercial CCK-8 assay kit (cat. no. CA1210; Beijing Solarbio Science & Technology Co., Ltd.). Cells were seeded in 96-well plates at a density of $4x10^3$ cells/well. After incubation for 0, 24, 48 and 72 h at 37˚C, 5% CO_2, 10 μl CCK-8 solution was added to each well and incubated for 2 h. The absorbance of the reactant at 450 nm was measured using a microplate reader (BioTek Instruments, Inc.).

Colony forming assay. A total of 500 cells were seeded in a petri dish and cultured in a condition of 37˚C with 5% CO_2. At 2 weeks later, cells were fixed with 4% paraformaldehyde for 15 min at room temperature. The number of cell colonies was then counted after staining by Wright-Giemsa stain (cat. no. DM0007; Beijing Leagene Biotech Co Ltd.) for 12 min at room temperature.

Wound-healing assay. Wound-healing assay was performed to assess the cell migration ability. Cells were cultured in a serum-free medium and treated with 1 μg/ml mitomycin C for 1 h. Scratches were made in each well using a 200 μl pipette tip. After culturing for 24 h, the migration distance of cells was recorded by an inverted microscope (Olympus Corporation).

Transwell assay. Transwell assay was performed to assess the cell invasion ability. Cells were pipetted into the top of the Transwell chambers, which were pre-treated with Matrigel for 2 h at 37˚C. The culture medium supplemented with 10% FBS was added to the bottom chambers. After incubating for 24 h, cells in the lower membrane were fixed with 4% paraformaldehyde for 25 min at room temperature, and then stained with 0.1% crystal violet for 5 min at room temperature. Cells were observed by a IX53 optical microscope (Olympus Corporation).

Glutamate and glutamine assays. According to the manufacturer's instructions, the contents of glutamine and glutamate were analyzed by a Glutamine Assay Kit (cat. no. A073-1; Nanjing Jiancheng Bioengineering Institute) and a Glutamate Assay Kit (cat. no. A074-1; Nanjing Jiancheng Bioengineering Institute), respectively.

Immunohistochemistry (IHC). Tissue sections (5 μm thick) were sequentially subjected to xylene and graded ethanol solution (100, 95, 85 and 75%) for dewaxing and rehydration, followed by treatment with antigen retrieval solution at 100˚C for 10 min. Subsequently, sections were incubated with 3% H_2O_2 for 15 min and then blocked with 1% bovine serum albumin (Sangon Biotech Co., Ltd.). After incubation with the primary antibodies anti-Ki67 (cat. no. A2094; 1:100; ABclonal Biotech Co., Ltd.) and anti-TRIM33 (cat. no. sc-101179; 1:100; Santa Cruz Biotechnology, Inc.) at 4˚C overnight, the sections were incubated with the HRP-Goat anti-Rabbit IgG secondary antibody (cat. no. 31460; 1:500; Thermo Fisher Scientific, Inc.) or HRP-Goat anti-Mouse IgG secondary antibody (cat. no. 31430; 1:500; Thermo Fisher Scientific, Inc.)

Table I. Correlation between TRIM33 expression and clinicopathological parameters of patients with endometrial carcinoma.

	TRIM33 expression level			
Clinical parameters	Low	High	Total	P-value
Age				0.339
≤62	27	21	48	
>62	15	18	33	
Menopause				0.889
Yes	36	33	69	
No	6	6	12	
FIGO stage				0.374
I/II	35	36	71	
III/IV	7	3	10	
Muscular invasion endomembrane				0.005[a]
≤1/2	16	27	43	
>1/2	26	12	38	
Differentiated degree				0.018[a]
Low	10	4	14	
Middle	16	8	24	
High	16	27	43	

[a]Statistically significant. TRIM33, tripartite motif containing 33; FIGO, Federation International of Gynecology and Obstetrics.

at 37˚C for 60 min and then stained with a DAB Horseradish Peroxidase Color Development Kit (cat. no. DAB-1031; MXB Biotechnologies). Finally, the sections were counter-stained with hematoxylin for 3 min at room temperature and observed by a BX53 optical microscope (Olympus Corporation).

For the evaluation of clinical IHC staining an established semi-quantitative approach [Histoscore (H-score)] was performed as previously described (19). Briefly, The H-score was calculated by both the intensity of staining and the percentage of TRIM33 positive cells in tumor cells. The average of H-score for all clinical cases was calculated using the following formula: H-score=[1 x (% of cells stained at intensity category 1) + 2 x (% of cells stained at intensity category 2) + 3 x (% of cells stained at intensity category 3)]. The intensity categories 1, 2 and 3 represent the weak (less than 1%), intermediate (0-49%) and strong staining (>49%) of TRIM33 in tumor cells, respectively. Cases with an H-score higher than the average score were regarded as high expression of TRIM33, while cases with an H-core equal or less than the average are considered as low expression.

Co-immunoprecipitation (Co-IP). HEC-1-A and AN3CA cells were collected and lysed in the cell lysis buffer for western and IP (cat. no. P0013, Beyotime Institute of Biotechnology). A BCA protein assay kit (Beyotime Institute of Biotechnology) was used to measure the protein concentration. Next, CO-IP assay was performed using a Pierce™ Co-IP Kit (cat. no. 26149, Thermo Fisher Scientific Inc.) according to the manufacturer's instructions. Briefly, anti-TRIM33 (cat. no. sc-101179; Santa Cruz Biotechnology, Inc.) or anti-c-Myc antibody (cat. no. 10828-1-AP; Proteintech Group, Inc.) was immobilized onto a spin column using coupling resin separately. Then, 500 μl cell lysates (1 μg protein/μl; Input) were added to the indicated spin column and kept on a rotator for 2 h at 37˚C, respectively. The spin columns were collected and incubated with 200 μl IP cell lysis buffer. After centrifuging (1,000 x g for 1 min at room temperature), washing with modified Dulbecco's PBS (pH 7.4) and eluting with elution buffer, the eluent was collected for immunoblotting by anti-TRIM33 and anti-c-Myc antibodies. Briefly, 20 μl electrophoretic loading solution was separated by 8 or 12% SDS-PAGE electrophoresis and transferred to the polyvinylidene difluoride membranes (MilliporeSigma). After blocking with 5% skimmed milk at room temperature for 1 h, the membranes were incubated with the primary antibodies anti-TRIM33 (cat. no. sc-101179, 1:300, Santa Cruz Biotechnology, Inc.) and anti-c-Myc (cat. no. 10828-1-AP, 1:1,000, Proteintech) at 4˚C overnight and then conjugated with the HRP-labeled Goat Anti-Mouse IgG secondary antibody (cat. no. A0216; 1:5,000; Beyotime Institute of Biotechnology) or HRP-labeled Goat Anti-Rabbit IgG (cat. no. A0208; 1:5,000; Beyotime Institute of Biotechnology) for 45 min at 37˚C. Subsequently, the protein bands were detected by ECL chemiluminescent substrate (cat. no. P0018; Beyotime Institute of Biotechnology) and observed by a gel image processing system (cat. no. WD-9413B; Beijing Liuyi Biotechnology Co., Ltd.).

Reverse transcription-quantitative (RT-q) PCR. Total RNA was extracted from tissues or $2x10^6$ cells using TRIpure reagent (RP1001, BioTeke, Beijing, China) according to the manufacturer's protocols. The concentration of the RNA was determined with a NANO 2000 spectrophotometer

(Thermo Fisher Scientific, Inc.). The BeyoRT II M-MLV reverse transcriptase (cat. no. D7160L; Beyotime Institute of Biotechnology) was used for reverse transcription according to the manufacturer's protocols. SYBR-Green PCR Master Mix (cat. no. PC1150; Beijing Solarbio Science & Technology Co., Ltd.) and the Exicycler 96 Real-Time PCR Detection System (Bioneer Corporation) were employed for RT-qPCR according to the manufacturer's protocols. The cycling conditions comprised an initial denaturation step for 5 min at 94˚C, followed by 40 cycles at 94˚C for 15 sec (denaturation) and annealing at 60˚C for 25 sec and elongation at 72˚C for 30 sec. The primers used were as follows: TRIM33 (forward: 5'-AAC CCAACGAGCCCTAC-3', reverse: 5'-TGAGCCAGCATC TTCCA-3'); solute carrier family 1 member 5 (SLC1A5; forward: 5'-CACTGCCTTTGGGACCTCT-3', reverse: 5'-CAG GATGAAACGGCTGATGT-3'); glutaminase (GLS; forward: 5'-CCAAAGTTCCCTTCTGT-3', reverse: 5'-CTTAGTCCA CTCGGCTC-3'); and c-Myc (forward: 5'-CACCCTTCTCCC TTCGG-3', reverse: 5'-CAGTCCTGGATGATGATGTTT-3'). The relative quantification of target genes in fresh-frozen tumor/normal endometrium tissues and the cultured EC cells was calculated by $2^{-\Delta Cq}$ and $2^{-\Delta\Delta Cq}$ methods (20), respectively. β-actin was used as an internal control.

c-Myc protein degradation assay. Prior to cell lysis, HEC-1-A cells were treated with CHX (50 μg/ml) for 0, 20, 40, 60 and 80 min to block new protein synthesis. Lv-Vector/Lv-TRIM33-OV infected HEC-1-A cells were treated with 50 μg/ml CHX for 80 min in the absence or presence of 20 μM MG132. MG132 was used to block proteasomal protein degradation. Then, the treated cells were subjected to western blot analysis to detect the expression of c-Myc protein, as described below.

Western blot analysis. Proteins were extracted from tissues or cells using the cell lysis buffer for western blotting and IP (cat. no. P0013; Beyotime Institute of Biotechnology). The protein concentration was determined using a BCA protein assay kit (cat. no. P0011, Beyotime Institute of Biotechnology). An equivalent amount of protein (40 μg) was separated by 8, 10 or 12% SDS-PAGE electrophoresis and transferred to the polyvinylidene difluoride membranes (MilliporeSigma). After blocking with 5% skimmed milk at room temperature for 1 h, the membranes were incubated with the primary antibodies anti-β-actin (cat. no. AF0003, 1:1,000; Beyotime Institute of Biotechnology), anti-TRIM33 (cat. no. sc-101179; 1:300; Santa Cruz Biotechnology, Inc.), anti-SLC1A5 (cat. no. AF6610; 1:1,000; Affinity Biosciences), anti-GLS (cat. no. DF13334, 1:1,000; Affinity Biosciences) or anti-c-Myc (cat. no. 10828-1-AP; 1:1,000; Proteintech Group, Inc.) at 4˚C overnight and then conjugated with the HRP-labeled Goat Anti-Rabbit IgG (cat. no. A0208; 1:5,000; Beyotime Institute of Biotechnology) or HRP-labeled Goat Anti-Mouse IgG secondary antibody (cat. no. A0216; 1:5,000; Beyotime Institute of Biotechnology) for 2 h at 37˚C. Subsequently, the protein bands were detected by ECL chemiluminescent substrate (Beyotime Institute of Biotechnology) and observed by the gel image processing system (cat. no. WD-9413B; Beijing Liuyi Biotechnology Co., Ltd.). The molecular weight marker was the PageRuler pre-stained protein ladder (10-180 kDa) from Thermo Fisher Scientific, Inc.

Animal model. A total of 25 female BALB/c nude mice (4-weeks old) were purchased from Cavensla Laboratory Animal Co., Ltd. All mice were housed in a 12-h light/dark cycle laboratory animal room of 22±1˚C and 45-55% humidity, with free access to food and water. According to the experimental protocol, the 25 mice were randomly divided into 5 groups (5 mice per group), TRIM33-overexpressed or -silenced HEC-1-A cells were injected into the subcutis of mice in the corresponding group. Tumor size was measured every 3 days and then calculated according to the formula: Tumor volume=0.5 x length x $(\text{width})^2$. At 24 days later, all the mice were humanely sacrificed via carbon dioxide inhalation (50% volume displacement/min) and the tumor tissues were excised for further analysis.

Statistical analysis. Statistical data was presented as mean ± SD. All analyses were performed using GraphPad Prism 9.0 (Dotmatics). The association between two categorical variables were compared using Chi-square test. Student's t-test or one-way ANOVA with Tukey's multiple comparisons test was used to compare groups for continuous variables. In addition, the public Tumor IMmune Estimation Resource database (TIMER2.0, http://timer.cistrome.org/) and UALCAN data portal (http://ualcan.path.uab.edu/analysis.html) were used to analyze the expression of TRIM33 in EC patients. $P<0.05$ was considered to indicate a statistically significant difference.

Results

Association between TRIM33 expression and the clinicopathological features of patients with EC. Data from the TIMER2.0 database and UALCAN data portal showed that TRIM33 was significantly downregulated in EC tissues (Fig. 1A and B). However, there was no significant correlation (P=0.25) between TRIM33 expression and patient outcome s (Fig. 1C). In addition, downregulation of TRIM33 was consistently observed in tumor tissues of patients with EC, regardless of age (Fig. 1D). Similar mRNA levels of TRIM33 were also detected in the collected EC tissues (Fig. 1E). In addition, it was found that the lower expression of TRIM33 in EC tissues was positively associated with the extensive muscle invasion and poor differentiation grade (Table I), but not with the age and the Federation International of Gynecology and Obstetrics (FIGO) stage (19). The representative images of IHC staining of TRIM33 in EC tissues are shown in Fig. 1F.

Effect of TRIM33 on EC cell proliferation, migration and invasion in vitro. To further investigate the role of TRIM33 in EC progress, TRIM33 overexpressed or silenced HEC-1-A and AN3CA cell lines were successfully constructed, as confirmed by the RT-qPCR and western blot assays (Fig. 2A). CCK-8 assay showed that cell viability was clearly decreased after TRIM33 overexpression but was increased after TRIM33 knockdown (Fig. 2B). Consistently, colony formation assay indicated that knockdown of TRIM33 promoted cell proliferation (Fig. 2C and D), whereas overexpression of TRIM33

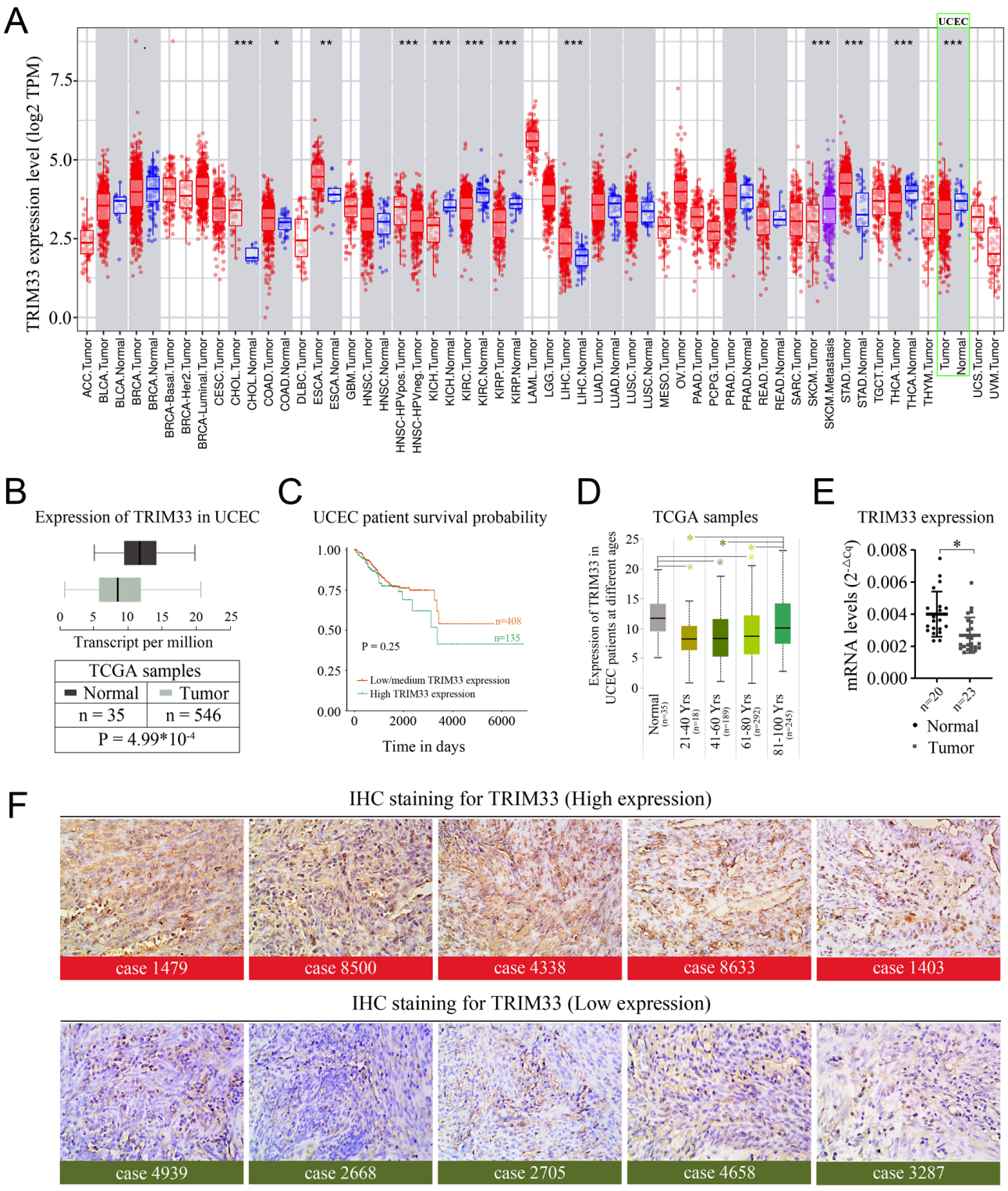

Figure 1. TRIM33 is downregulated in tumor samples of patients with EC. (A) The expression of TRIM33 in pan-cancer accessible at the Tumor IMmune Estimation Resource database (https://cistrome.shinyapps.io/timer/). TRIM33 expression in UCEC is highlighted by the green rectangle. (B) TRIM33 expression levels in normal and EC tumor samples. Data was derived from UALCAN website (https://ualcan.path.uab.edu/analysis.html) based on The Cancer Genome Atlas database. (C) Relationship between TRIM33 levels and the survival probabilities of patients with UCEC (data source, UALCAN). (D) The expression of TRIM33 in UCEC patients at different ages (data source, UALCAN). (E) Expression of TRIM33 at mRNA level in collected 20 normal endometrial tissues and 23 EC tumor samples. (F) Immunohistochemical staining for TRIM33 in EC tissues; five representative images for high and low TRIM33 expression, respectively (magnification, x400). EC, endometrial carcinoma. *P<0.05; **P<0.01; ***P<0.001 and $^{@}$P<0.05. TRIM33, tripartite motif containing 33; UCEC, uterine corpus endometrial carcinoma; EC, endometrial carcinoma; IHC, immunohistochemistry; TCGA, The Cancer Genome Atlas database.

inhibited cell proliferation (Fig. 2C and E). Next, results of wound healing (Fig. 3A-C) and Transwell assays (Fig. 3D-F) suggested that downregulation of TRIM33 enhanced the migration and invasion abilities of HEC-1-A and AN3CA

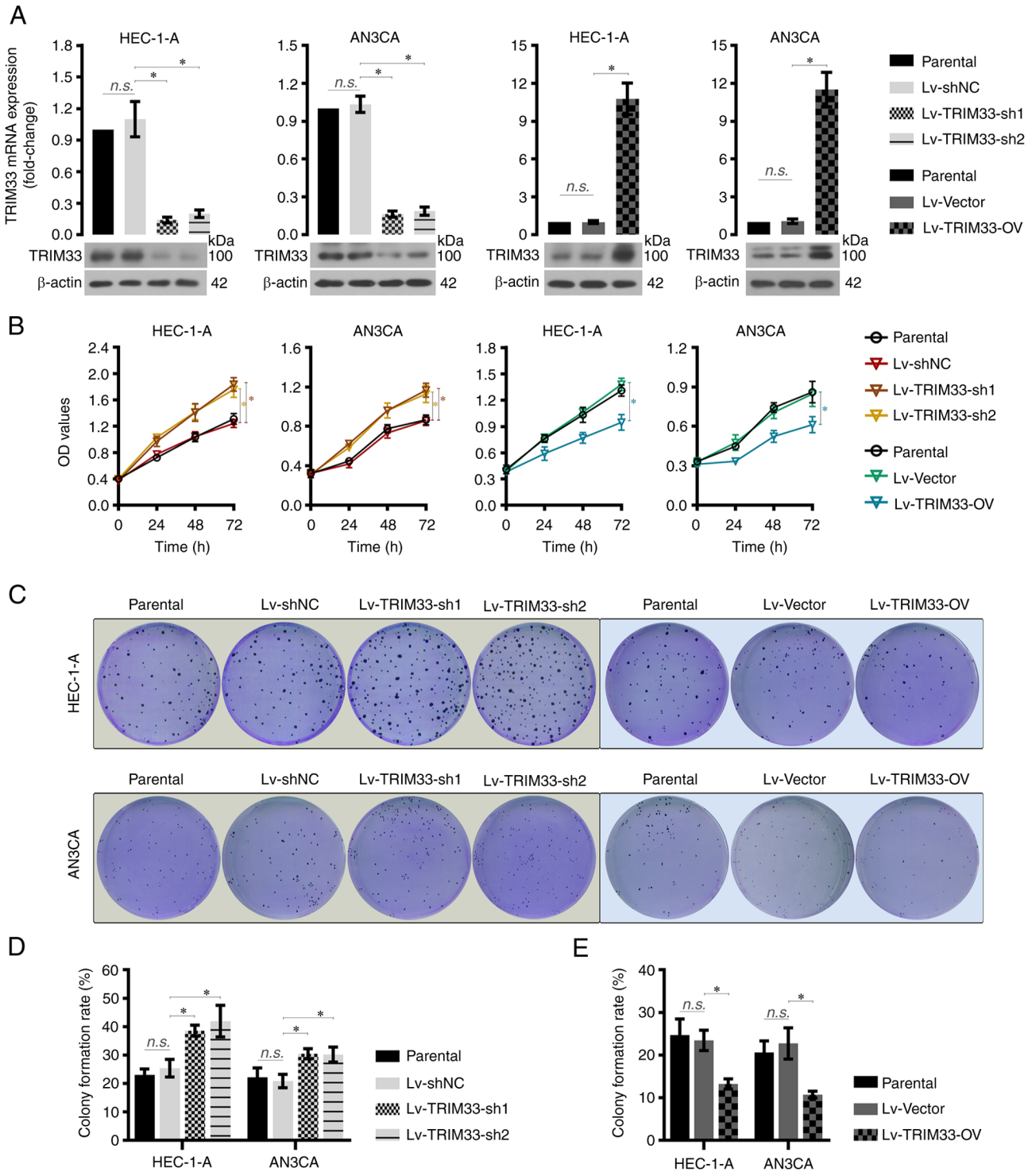

Figure 2. TRIM33 overexpression inhibits HEC-1-A and AN3CA cell proliferation *in vitro*. (A) Reverse transcription-quantitative PCR and western blotting were used to detect the expression of TRIM33 in TRIM33-silenced or -overexpressed EC cells. (B) Analysis of cell viability by CCK-8 assay. (C-E) Colony formation assay was performed to evaluate the colony formation capacity of EC cells. *P<0.05; n.s., no significance. TRIM33, tripartite motif containing 33; EC, endometrial carcinoma; Lv, lentivirus vector; sh, short hairpin; NC, negative control, OV, overexpression.

cells. By contrast, upregulation of TRIM33 could inhibit cell migration and invasion.

Effect of TRIM33 on glutamine metabolism of EC cell in vitro. The present study also found that overexpression of TRIM33 significantly inhibited the glutamine uptake and intracellular glutamate production in HEC-1-A and AN3CA cells, whereas TRIM33 knockdown resulted in the opposite effects (Fig. 4A and B). As a well-known sodium-dependent glutamine transporter, an increase of SLC1A5 was observed in TRIM33-silenced cells (Fig. 4C), but a decrease in TRIM33-overexpressed cells (Fig. 4D). Meanwhile, RT-qPCR and western blot assays also confirmed that GLS, a key amidohydrolase in the rate-limiting step of glutamine-based

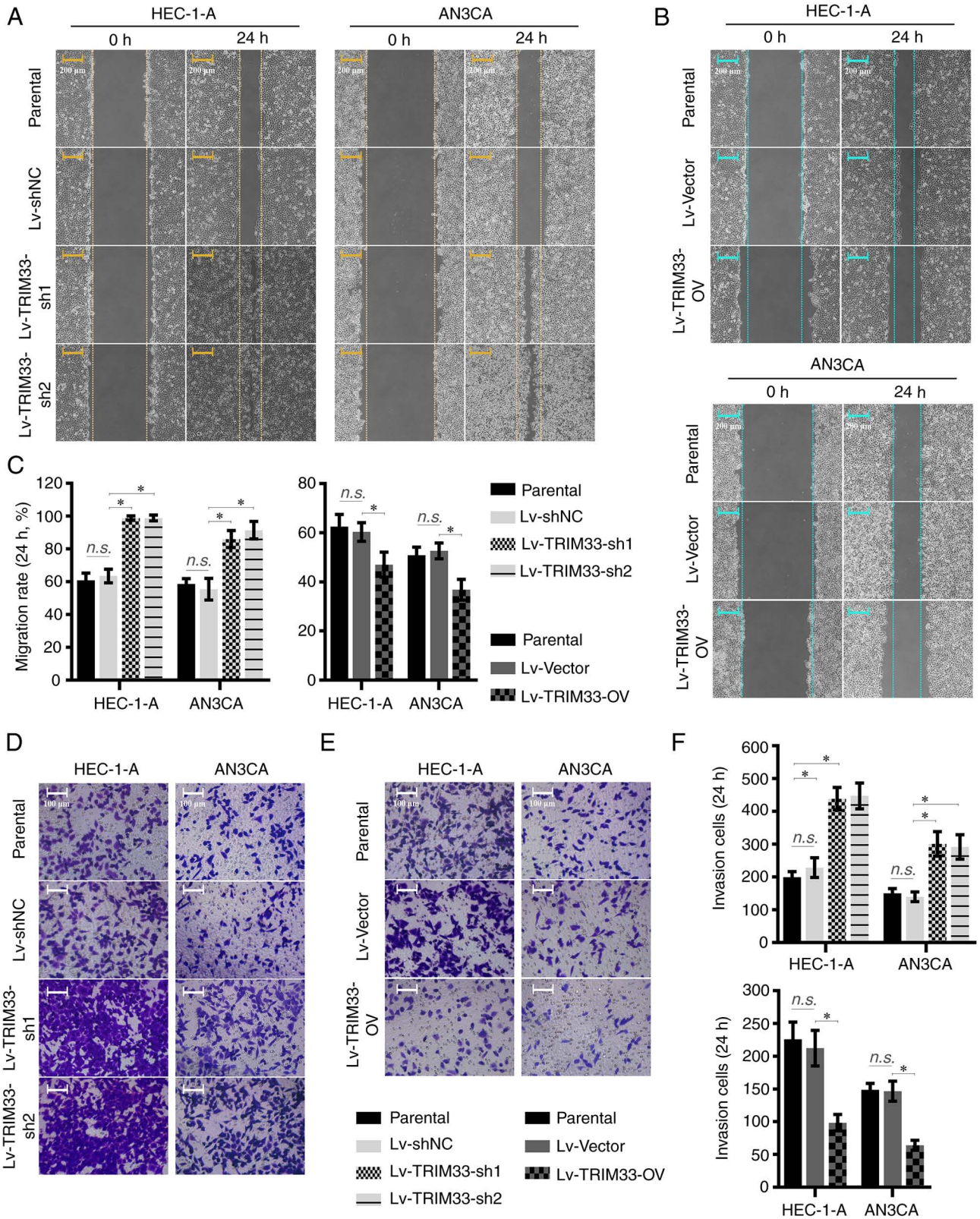

Figure 3. TRIM33 overexpression inhibits HEC-1-A and AN3CA cell migration and invasion *in vitro*. (A and B) Migration abilities of TRIM33-silenced or -overexpressed EC cells were determined by wound healing scratch assay. (C) Quantitative analysis of migrated HEC-1-A and AN3CA cells. (D and E) Cell invasion abilities were analyzed by Transwell assay. (F) Quantitative analysis of invaded HEC-1-A and AN3CA cells. *P<0.05; n.s., no significance. TRIM33, tripartite motif containing 33; EC, endometrial carcinoma; Lv, lentivirus vector; sh, short hairpin; NC, negative control, OV, overexpression.

anaplerosis (21), was consistently upregulated after TRIM33 knockdown but downregulated after TRIM33 overexpression (Fig. 4C and D).

c-Myc mediates the effect of TRIM33 on EC cell in vitro. Furthermore, the expression of c-Myc in HEC-1-A and AN3CA cells was clearly downregulated following TRIM33

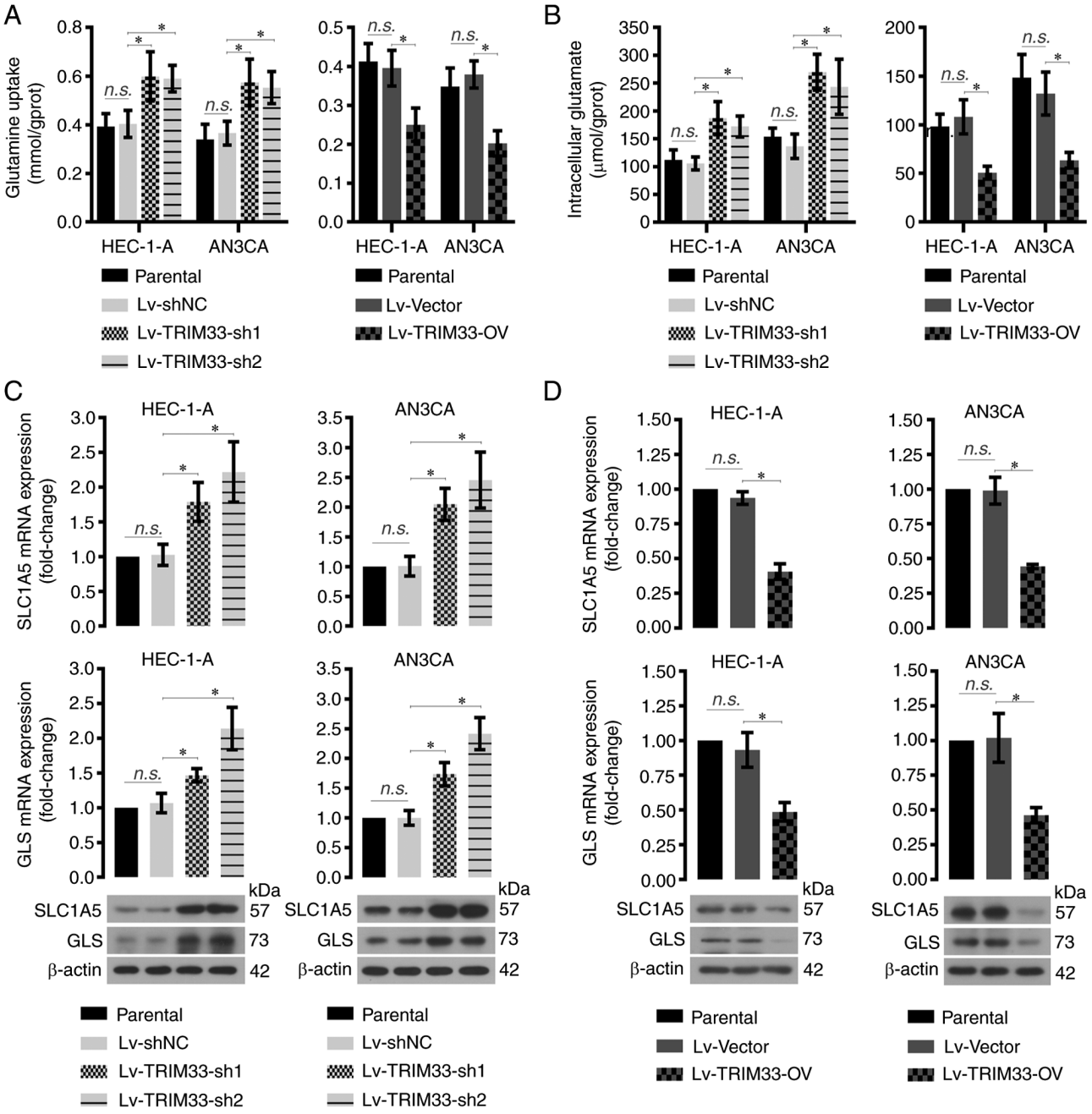

Figure 4. TRIM33 overexpression inhibits the glutamine metabolism in HEC-1-A and AN3CA cells *in vitro*. (A) Glutamine uptake and (B) intracellular glutamate production of TRIM33-silenced or -overexpressed EC cells were analyzed using the commercial kits. (C and D) Reverse transcription-quantitative PCR and western blotting were used to detect the expression of SLC1A5 and GLS in EC cells. *P<0.05; n.s., no significance. TRIM33, tripartite motif containing 33; EC, endometrial carcinoma; SLC1A5, Solute Carrier Family 1 Member 5; GLS, glutaminase; Lv, lentivirus vector; sh, short hairpin; NC, negative control; OV, overexpression.

overexpression, but upregulated following TRIM33 knockdown (Fig. 5A and B). In addition, the interaction between TRIM33 and c-Myc was verified in HEC-1-A and AN3CA cells by Co-IP assay (Fig. 5C). As shown in Fig. 5D, TRIM33 inhibited c-Myc expression at the protein level and blockade of new protein synthesis by cycloheximide (CHX) suggested that TRIM33 expression inhibited the stability of c-Myc. MG132 was then used to block proteasomal protein degradation. Compared with the negative control group (Lv-Vector group), cells with forced TRIM33 expression expressed comparable level of c-Myc in the presence of MG132 (Fig. 5E). To verify whether c-Myc was the intermediate factor between TRIM33 and ER cell growth, overexpression of c-Myc (Ov-c-Myc) in HEC-1-A cells was constructed by plasmid transfection (Fig. 5F). Further analysis of CCK-8 (Fig. 5G) and Transwell (Fig. 5H) results showed that overexpression of c-Myc partially reversed the inhibitory effects of TRIM33 on the viability and invasiveness of HEC-1-A cells. Additionally, c-Myc overexpression also promoted the production of intracellular glutamate in cells with forced TRIM33 expression (Fig. 5I; Lv-TRIM33-OV+Ov-c-Myc group vs. Lv-TRIM33-OV+Ov-Vector group), suggesting that c-Myc was an important factor in the TRIM33-glutamine regulatory axis.

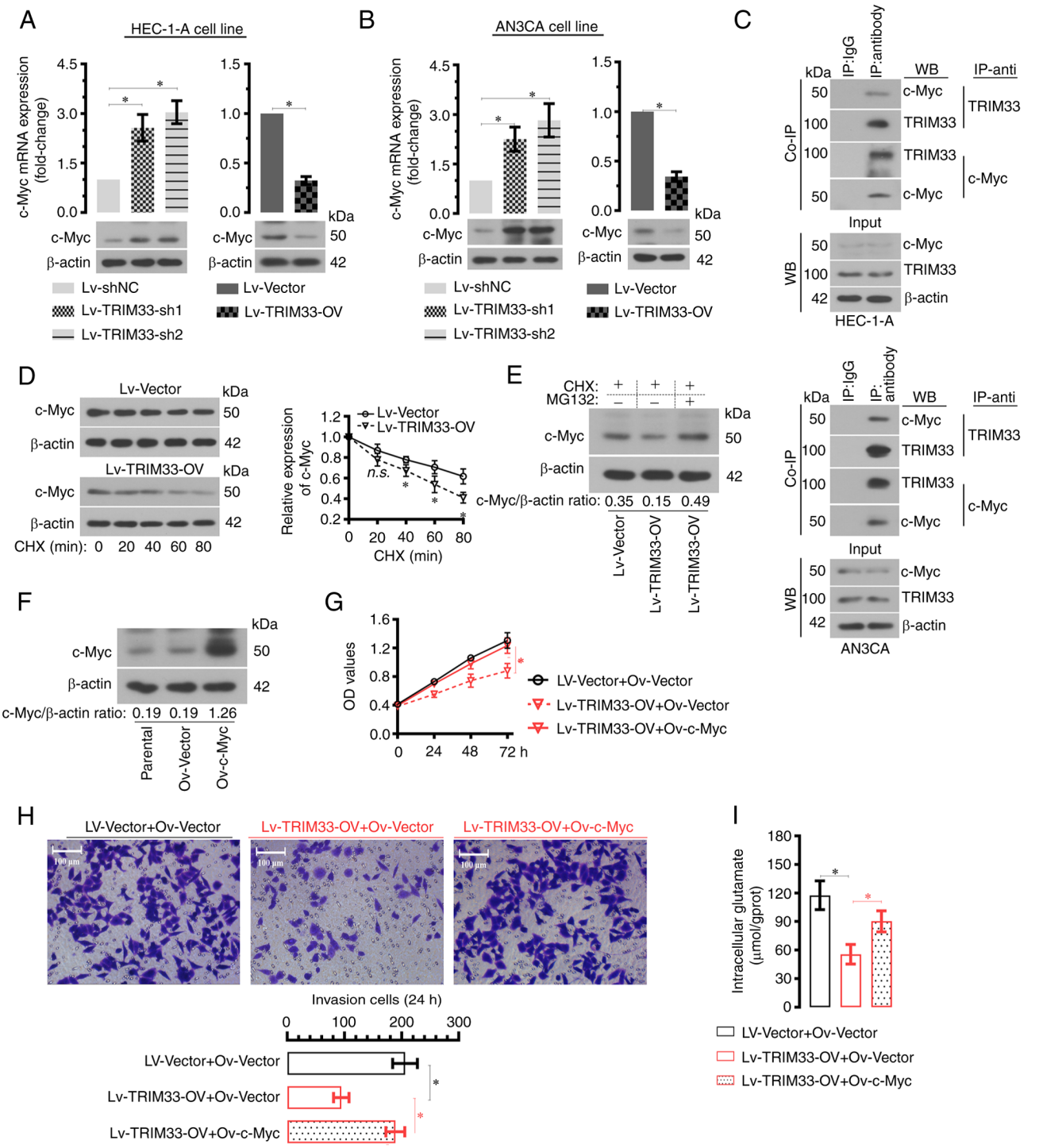

Figure 5. Effects of TRIM33 on EC cell malignant phenotypes may be related to its negative regulation of c-Myc. (A and B) Reverse transcription-quantitative PCR and western blot assay were performed to detect the expression of c-Myc in TRIM33-silenced or -overexpressed HEC-1-A and AN3CA cells. (C) Co-IP assays of the interaction between TRIM33 and c-Myc in HEC-1-A and AN3CA cells. (D) The effect of TRIM33 overexpression on c-Myc protein degradation was investigated in HEC-1-A cells treated with CHX (50 μg/ml). (E) Lv-Vector/Lv-TRIM33-OV infected HEC-1-A cells were treated with CHX (50 μg/ml) for 80 min in the absence or presence of MG132 (20 μM). c-Myc expression was analyzed by western blotting. (F) Western blotting for c-Myc expression in parental and Lv-Vector/Lv-TRIM33-OV infected HEC-1-A cells. (G) CCK-8 assay was performed to evaluate the viability of HEC-1-A cells. (H) The invasive ability of HEC-1-A cells was analyzed by Transwell assay. (I) Intracellular glutamate production of HEC-1-A cells was analyzed by using a commercial kit. EC, endometrial carcinoma. *P<0.05; n.s., no significance. TRIM33, tripartite motif containing 33; EC, endometrial carcinoma; Co-IP, co-immunoprecipitation; CHX, cycloheximide; Lv, lentivirus vector; sh, short hairpin; NC, negative control; OV, overexpression.

Effect of TRIM33 on the tumorigenicity of HEC-1-A cells in vivo. Considering the anti-tumor effects of TRIM33 *in vitro*, EC model in BALB/c nude mice was constructed by subcutaneous injection of HEC-1-A cells. As shown in Fig. 6A, cells with TRIM33 knockdown exhibited a clear faster growth rate than cells with TRIM33 overexpression. Similar differences were also observed in tumor weight between the TRIM33-overexpressed and -silenced groups

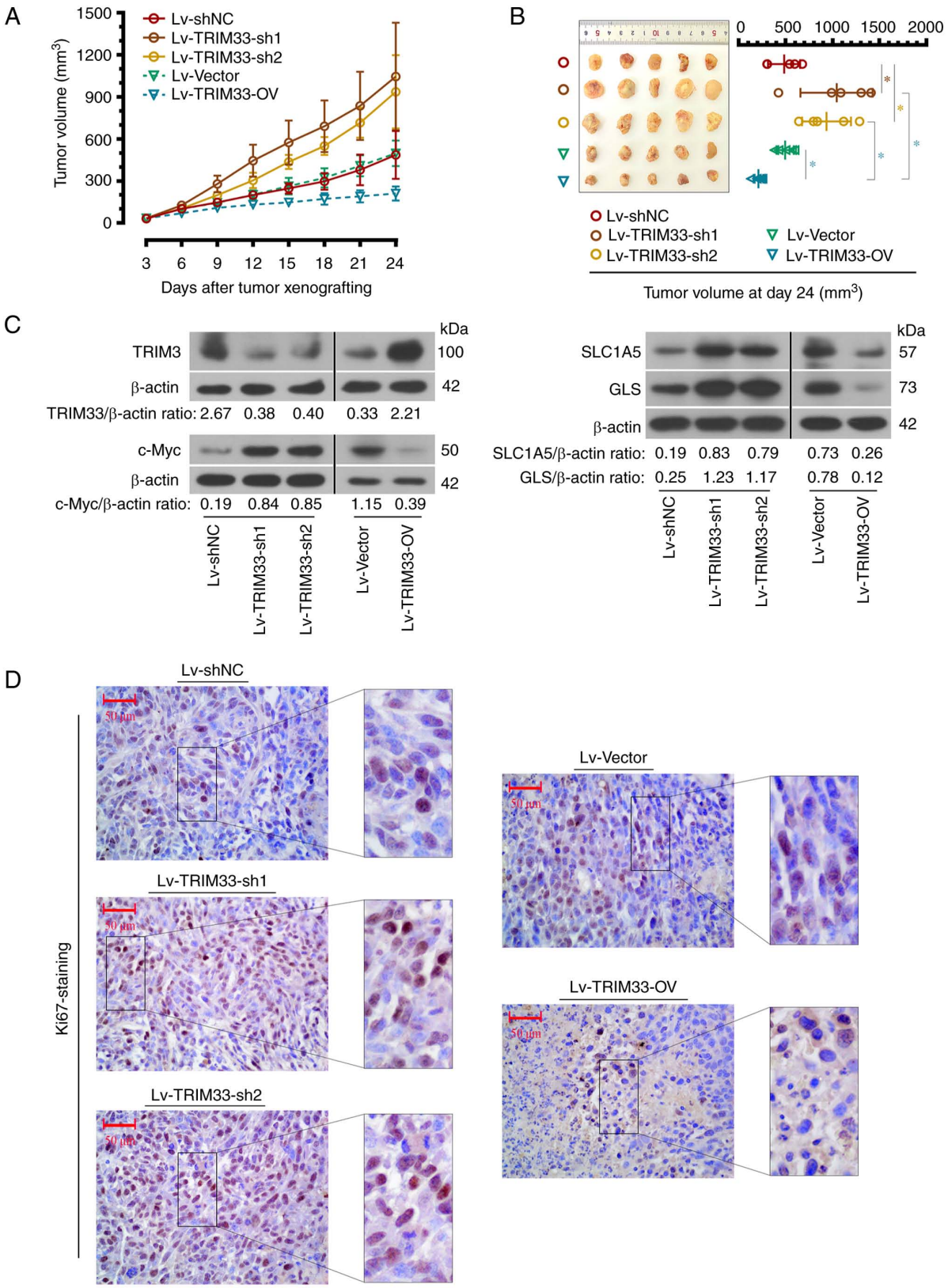

Figure 6. Effects of TRIM33 on HEC-1-A cell growth *in vivo*. (A) Tumor volume was recorded every 3 days during the experiment. (B) Tumor picture and the end-point tumor volume at day 24 in HEC-1-A xenografts. (C) Western blotting was used to detect the expression of TRIM33, c-Myc, SLC1A5 and GLS in the tumor tissues from mice in different groups. (D) Ki67 expression in the tumor tissues were evaluated by using immunohistochemical staining. *P<0.05; n.s., no significance. TRIM33, tripartite motif containing 33; SLC1A5, Solute Carrier Family 1 Member 5; GLS, glutaminase Lv, lentivirus vector; sh, short hairpin; NC, negative control; OV, overexpression.

(Fig. 6B; Lv-TRIM33-sh1 or Lv-TRIM33-sh2 groups vs. Lv-TRIM33-OV group). In lines with the *in vitro* experimental results, TRIM33 knockdown resulted in the clear increase of c-Myc, SLC1A5 and GLS, whereas TRIM33 overexpression

prominently inhibited these protein expressions (Fig. 6C). In addition, the expression of Ki67, a common cell proliferation-related molecule, in TRIM33-overexpressed group was weaker than that of TRIM33-silenced groups (Fig. 6D).

Discussion

The TRIM33 gene is on human chromosome 1p13 and belongs to a sub-family of chromatin binding TRIM proteins. The abnormal expression of TRIM33 is associated with the occurrence of human diseases, such as psoriasis (22), myocardial fibrosis (23) and types of cancer (24). The current study is the first, to the best of the authors' knowledge, to demonstrate that TRIM33 could suppress EC cell proliferation, migration and invasion and that these effects were dependent on inhibition of c-Myc, which is often highly expressed and serves pro-survival activity in cancer cells (17,18). In addition, the present study highlighted that the link between TRIM33 and glutamine metabolism in EC indeed exists.

Glutamine is a nutrient that supports cell energy production and biomass synthesis; it has been established that an important metabolic adaptation of cancer cells is their propensity to exhibit increased glutamine consumption (25), with some cancer cells dying rapidly with glutamine depletion. For example, deprivation of glutamine potently inhibited neuroblastoma cell proliferation and induced apoptosis (26). The present study found that TRIM33 could inhibit the glutamine uptake and intracellular glutamate production in EC cells by downregulating the levels of SLC1A5 and GLS. SLC1A5, a sodium-dependent amino acids transporter, accepts as substrates all neutral amino acids such as glutamine (27). Downregulation of SLC1A5 results in a decrease of spheroid cross-sectional area in EC cells, suggesting a reliance on SLC1A5-mediated glutamine uptake (28). In accordance with this, the present study showed that upregulation of TRIM33 significantly suppressed SLC1A5 and GLS expression in HEC-1-A and AN3CA cells. GLS is a phosphate-activated amidohydrolase that catalyzes the cleavage of the γ-nitrogen of glutamine, which is a rate-limiting step of glutamine-based anaplerosis (21). A previous study suggested that GLS-specific inhibitor bis-2-(5-phenylacetamido-1,3,4-thiadiazol-2-yl) ethyl sulfide treatment could blunt tumor progression in a mouse model of hepatocellular carcinoma (29). Accordingly, it was hypothesized that TRIM33 might inhibit the proliferation, migration and invasion of EC cells via regulation of glutamine metabolism.

Notably, glutamine is a crucial donor of reduced nitrogen for synthesis of purine and pyrimidines in proliferating mammalian cells (30-32) and thus participates in regulation of cell cycle progression. Gaglio *et al* (25) demonstrated that reduction or complete depletion of glutamine in K-ras transformed fibroblasts caused a slower re-entry of synchronized cells into the cell cycle. However, the present study did not elucidate whether TRIM33 regulates the cell cycle by affecting the glutamine metabolic pathway, thereby accelerating cancer cell apoptosis. In addition, the increased glutamine uptake that is common in types of cancer has been proved to strongly stimulate mTOR activity (33). Due to the contribution of mTOR pathway activation in the progression of EC, further work will be needed to investigate the relationship among TRIM33, glutamine metabolism and mTOR pathway in future EC development.

c-Myc was initially identified as a helix-loop-helix leucine zipper oncogenic transcription factor that played a crucial role in DNA replication (34). It was subsequently confirmed that c-Myc could directly activate several components of the glucose metabolic pathway to deregulate glycolysis (35). The present study demonstrated that TRIM33 acted as a tumor suppressor in EC by reducing the protein stability of c-Myc. Wise *et al* (36) demonstrated that oncogenic levels of c-Myc induces the addiction of proliferating cells to glutamine, a bioenergetic substrate, to maintain survival. In addition, proteomic analysis of mitochondria of human B lymphocytes with forced c-Myc expression revealed that c-Myc enhances the expression of glutamine metabolism-related enzyme (17). A consequence of this c-Myc-dependent glutaminolysis is that c-Myc could directly inhibit the microRNAs (miR-23a and miR-23b) that targeted the 3'-UTR of GLS mRNA. Hence, it was hypothesized that TRIM33, acting as an E3 ubiquitin ligase, could inhibit glutamine metabolism in EC cells via promoting c-Myc protein degradation. Notably, there is evidence that endogenous TRIM33 levels are inversely correlated with β-catenin in human glioblastoma specimens, specifically, that TRIM33 suppresses tumorigenesis by degrading nuclear β-catenin (37). It is widely known that aberrant increase in abundance of nuclear β-catenin triggers upregulation of proto-oncogenes such as c-Myc, which is hypothesized to be the basis for tumorigenesis (38). Thus, apart from directly interacting with and ubiquitylating c-Myc, TRIM33 may also affect c-Myc by regulating β-catenin signaling and thus play a role in EC progression, which deserves further study.

Additionally, the present study was based on such a limited number of samples and experiments. In the future, larger patient cohorts and additional functional assays could be performed to enhance the understanding of the biological role of TRIM33 and its feasibility in the diagnosis and treatment of EC. For example, evidence has been provided that increased or prolonged exposure to estrogen of the uterus is positively related to risk of EC development (39). Zhou *et al* (40) reported that estrogen significantly accelerates the glutamine metabolism in estrogen-dependent EC cells and this effect is partially mediated by the expression of c-Myc. Since the present study demonstrated that TRIM33 inhibited glutamine metabolism by suppressing c-Myc protein expression, the links between TRIM33 and glutamine metabolism in clinical EC patients, especially in the estrogen-dependent type, clearly merits further study.

In brief, the present study evaluated the potential effects of TRIM33 on cell viability and tumor growth in human EC cells (HEC-1-A and AN3CA) and a BALB/c nude mice mouse model of HEC-1-A. It demonstrated that TRIM33 suppressed *in vitro* malignant phenotypes of EC cells and *in vivo* tumor growth by promoting c-Myc protein degradation and glutamine metabolism. These findings provide a scientific basis that TRIM33 maybe a potential target for EC treatment.

Acknowledgments

Not applicable.

Funding

Not applicable.

Availability of data and materials

The datasets used and/or analyzed during the current study are available from the corresponding author on reasonable request.

Authors' contributions

YQ and NM were responsible for conceptualization, methodology, data analysis, writing the original draft and reviewing the manuscript. YQ, NM and JZ performed the experiments. JZ helped with writing the original draft, mining and analyzing databases. YQ and NM confirm the authenticity of all the raw data. All authors read and approved the final version of the manuscript.

Ethics approval and consent to participate

Informed consent was obtained from the participants. All experiments performed in this study were completed in accordance with the *Declaration of Helsinki* as revised in 2013 and approved by the ethics committee of Shengjing Hospital of China Medical University (approval no. 2018PS251K).

All animal experiments were approved by the Animal Ethics Committee of Shengjing Hospital of China Medical University [approval no. 2021PS343K(X1)] and complied with the ARRIVE guidelines and the AVMA euthanasia guidelines 2020. For the *in vivo* EC model, the tumor burden did not exceed the recommendations of the University of Pennsylvania Institutional Animal Care and Use Committee guidelines.

Patient consent for publication

Informed consent was obtained for the publication of clinical data.

Competing interests

The authors declare that they have no competing interests.

Reference

1. Williams E, Villar-Prados A, Bowser J, Broaddus R and Gladden AB: Loss of polarity alters proliferation and differentiation in low-grade endometrial cancers by disrupting Notch signaling. PLoS One 12: e0189081, 2017.
2. 2.Siegel RL, Miller KD, Fuchs HE and Jemal A: Cancer statistics, 2022. CA Cancer J Clin 72: 7-33, 2022.
3. Hatakeyama S: TRIM proteins and cancer. Nat Rev Cancer 11: 792-804, 2011.
4. Kulkarni A, Oza J, Yao M, Sohail H, Ginjala V, Tomas-Loba A, Horejsi Z, Tan AR, Boulton SJ and Ganesan S: Tripartite Motif-containing 33 (TRIM33) protein functions in the poly(ADP-ribose) polymerase (PARP)-dependent DNA damage response through interaction with Amplified in Liver Cancer 1 (ALC1) protein. J Biol Chem 288: 32357-32369, 2013.
5. Sedgwick GG, Townsend K, Martin A, Shimwell NJ, Grand RJ, Stewart GS, Nilsson J and Turnell AS: Transcriptional intermediary factor 1γ binds to the anaphase-promoting complex/cyclosome and promotes mitosis. Oncogene 32: 4622-4633, 2013.
6. Bai X, Kim J, Yang Z, Jurynec MJ, Akie TE, Lee J, LeBlanc J, Sessa A, Jiang H, DiBiase A, *et al*: TIF1gamma controls erythroid cell fate by regulating transcription elongation. Cell 142: 133-143, 2010.
7. Chen M, Lingadahalli S, Narwade N, Lei KMK, Liu S, Zhao Z, Zheng Y, Lu Q, Tang AHN, Poon TCW and Cheung E: TRIM33 drives prostate tumor growth by stabilizing androgen receptor from Skp2-mediated degradation. EMBO Rep 23: e53468, 2022.
8. Herquel B, Ouararhni K, Khetchoumian K, Ignat M, Teletin M, Mark M, Béchade G, Van Dorsselaer A, Sanglier-Cianférani S, Hamiche A, *et al*: Transcription cofactors TRIM24, TRIM28, and TRIM33 associate to form regulatory complexes that suppress murine hepatocellular carcinoma. Proc Natl Acad Sci USA 108: 8212-8217, 2011.
9. Xu Y, Wu G, Zhang J, Li J, Ruan N, Zhang J, Zhang Z, Chen Y, Zhang Q and Xia Q: TRIM33 overexpression inhibits the progression of clear cell renal cell carcinoma in vivo and in vitro. Biomed Res Int 2020: 8409239, 2020.
10. Dang CV, Le A and Gao P: MYC-induced cancer cell energy metabolism and therapeutic opportunities. Clin Cancer Res 15: 6479-6483, 2009.
11. Hoffman B and Liebermann DA: Apoptotic signaling by c-MYC. Oncogene 27: 6462-6472, 2008.
12. Zhang Q, Xu P, Lu Y and Dou H: Correlation of MACC1/c-Myc expression in endometrial carcinoma with clinical/pathological features or prognosis. Med Sci Monit 24: 4738-4744, 2018.
13. Hawksworth D, Ravindranath L, Chen Y, Furusato B, Sesterhenn IA, McLeod DG, Srivastava S and Petrovics G: Overexpression of C-MYC oncogene in prostate cancer predicts biochemical recurrence. Prostate Cancer Prostatic Dis 13: 311-315, 2010.
14. Chen CH, Shen J, Lee WJ and Chow SN: Overexpression of cyclin D1 and c-Myc gene products in human primary epithelial ovarian cancer. Int J Gynecol Cancer 15: 878-883, 2005.
15. Rochlitz CF, Herrmann R and de Kant E: Overexpression and amplification of c-myc during progression of human colorectal cancer. Oncology 53: 448-454, 1996.
16. Llombart V and Mansour MR: Therapeutic targeting of 'undruggable' MYC. EBioMedicine 75: 103756, 2022.
17. Gao P, Tchernyshyov I, Chang TC, Lee YS, Kita K, Ochi T, Zeller KI, De Marzo AM, Van Eyk JE, Mendell JT and Dang CV: c-Myc suppression of miR-23a/b enhances mitochondrial glutaminase expression and glutamine metabolism. Nature 458: 762-765, 2009.
18. Bott AJ, Peng IC, Fan Y, Faubert B, Zhao L, Li J, Neidler S, Sun Y, Jaber N, Krokowski D, *et al*: Oncogenic Myc induces expression of glutamine synthetase through promoter demethylation. Cell Metab 22: 1068-1077, 2015.
19. Lee HH, Wang YN, Xia W, Chen CH, Rau KM, Ye L, Wei Y, Chou CK, Wang SC, Yan M, *et al*: Removal of N-Linked Glycosylation Enhances PD-L1 Detection and Predicts Anti-PD-1/PD-L1 Therapeutic Efficacy. Cancer Cell 36: 168-178. e4, 2019.
20. Livak KJ and Schmittgen TD: Analysis of relative gene expression data using real-time quantitative PCR and the 2(-Delta Delta C(T)) Method. Methods 25: 402-408, 2001.
21. Cassago A, Ferreira AP, Ferreira IM, Fornezari C, Gomes ER, Greene KS, Pereira HM, Garratt RC, Dias SM and Ambrosio AL: Mitochondrial localization and structure-based phosphate activation mechanism of Glutaminase C with implications for cancer metabolism. Proc Natl Acad Sci USA 109: 1092-1097, 2012.
22. Zhang J, Zhu J, Chen X, Xia H and Yang L: E3 ubiquitin ligase Trim33 ubiquitylates Annexin A2 to promote NF-κB induced skin inflammation in psoriasis. J Dermatol Sci 107: 160-168, 2022.
23. Wei T, Du Y, Shan T, Chen J, Shi D, Yang T, Wang J, Zhang J and Li Y: The crystallin alpha B (HSPB5)-tripartite motif containing 33 (TRIM33) axis mediates myocardial fibrosis induced by angiotensinogen II through transforming growth factor-β (TGF-β1)-Smad3/4 signaling. Bioengineered 13: 8836-8849, 2022.
24. Shen Q, He T and Yuan H: Hsa_circ_0002577 promotes endometrial carcinoma progression via regulating miR-197/CTNND1 axis and activating Wnt/β-catenin pathway. Cell Cycle 18: 1229-1240, 2019.
25. Gaglio D, Soldati C, Vanoni M, Alberghina L and Chiaradonna F: Glutamine deprivation induces abortive s-phase rescued by deoxyribonucleotides in k-ras transformed fibroblasts. PLoS One 4: e4715, 2009.

26. Qing G, Li B, Vu A Skuli N, Walton ZE, Liu X, Mayes PA, Wise DR, Thompson CB, Maris JM, *et al*: ATF4 regulates MYC-mediated neuroblastoma cell death upon glutamine deprivation. Cancer Cell 22: 631-644, 2012.
27. Li J, Wang X, Su Y, Hu S and Chen J: TRIM33 Modulates Inflammation and Airway Remodeling of PDGF-BB-Induced Airway Smooth-Muscle Cells by the Wnt/β-Catenin Pathway. Int Arch Allergy Immunol 183: 1127-1136, 2022.
28. Marshall AD, van Geldermalsen M, Otte NJ, Lum T, Vellozzi M, Thoeng A, Pang A, Nagarajah R, Zhang B, Wang Q, *et al*: ASCT2 regulates glutamine uptake and cell growth in endometrial carcinoma. Oncogenesis 6: e367, 2017.
29. Xiang Y, Stine ZE, Xia J, Lu Y, O'Connor RS, Altman BJ, Hsieh AL, Gouw AM, Thomas AG, Gao P, *et al*: Targeted inhibition of tumor-specific glutaminase diminishes cell-autonomous tumorigenesis. J Clin Invest 125: 2293-2306, 2015.
30. Zhang J, Pavlova NN and Thompson CB: Cancer cell metabolism: The essential role of the nonessential amino acid, glutamine. EMBO J 36: 1302-1315, 2017.
31. Sullivan LB, Gui DY, Hosios AM, Bush LN, Freinkman E and Vander Heiden MG: Supporting aspartate biosynthesis is an essential function of respiration in proliferating cells. Cell 162: 552-563, 2015.
32. Birsoy K, Wang T, Chen WW, Freinkman E, Abu-Remaileh M and Sabatini DM: An essential role of the mitochondrial electron transport chain in cell proliferation is to enable aspartate synthesis. Cell 162: 540-551, 2015.
33. Laplante M and Sabatini DM: mTOR signaling in growth control and disease. Cell 149: 274-293, 2012.
34. Dominguez-Sola D, Ying CY, Grandori C, Ruggiero L, Chen B, Li M, Galloway DA, Gu W, Gautier J and Dalla-Favera R: Non-transcriptional control of DNA replication by c-Myc. Nature 448: 445-451, 2007.
35. Osthus RC, Shim H, Kim S, Li Q, Reddy R, Mukherjee M, Xu Y, Wonsey D, Lee LA and Dang CV: Deregulation of glucose transporter 1 and glycolytic gene expression by c-Myc. J Biol Chem 275: 21797-21800, 2000.
36. Wise DR, DeBerardinis RJ, Mancuso A, Sayed N, Zhang XY, Pfeiffer HK, Nissim I, Daikhin E, Yudkoff M, McMahon SB and Thompson CB: Myc regulates a transcriptional program that stimulates mitochondrial glutaminolysis and leads to glutamine addiction. Proc Natl Acad Sci USA 105: 18782-18787, 2008.
37. Xue J, Chen Y, Wu Y, Wang Z, Zhou A, Zhang S, Lin K, Aldape K, Majumder S, Lu Z and Huang S: Tumour suppressor TRIM33 targets nuclear β-catenin degradation. Nat Commun 6: 6156, 2015.
38. Anastas JN and Moon RT: WNT signalling pathways as therapeutic targets in cancer. Nat Rev Cancer 13: 11-26, 2013.
39. Veliça P, Davies NJ, Rocha PP, Schrewe H, Ride JP and Bunce CM: Lack of functional and expression homology between human and mouse aldo-keto reductase 1C enzymes: Implications for modelling human cancers. Mol Cancer 8: 121, 2009.
40. Zhou WJ, Zhang J, Yang HL, Wu K, Xie F, Wu JN, Wang Y, Yao L, Zhuang Y, Xiang JD, *et al*: Estrogen inhibits autophagy and promotes growth of endometrial cancer by promoting glutamine metabolism. Cell Commun Signal 17: 99, 2019.